Photomediated Solid-State Cross-Linking of an Elastin−Mimetic Recombinant Protein Polymer

Karthik Nagapudi,[†] William T. Brinkman,[†] Johannes E. Leisen,[‡] Lei Huang,[†] R. Andrew McMillan,[§] Robert P. Apkarian,[§] Vincent P. Conticello,[§] and Elliot L. Chaikof*[,†,⊥,#]

Departments of Surgery, Bioengineering, and Chemistry, Emory University, Atlanta, Georgia 30322, and School of Textile Engineering and Chemical Engineering, Georgia Institute of Technology, Atlanta, Georgia 30332

Received August 8, 2001

ABSTRACT: Solid-state cross-linking of elastin−mimetic fibers was investigated. Through available lysine residues, an elastin−mimetic protein polymer, poly((Val-Pro-Gly-Val-Gly)$_4$(Val-Pro-Gly-Lys-Gly))$_{39}$, was modified to incorporate an acrylate moiety. The degree of acrylate functionalization could be varied by changing the reactant ratio of anhydride to elastin. Acrylate modified elastomeric (AME) proteins were associated with lower inverse transition temperatures than the unmodified recombinant protein. The inverse transition temperature in turn dictated the temperature for fiber formation. Fibers and fabric samples of AME were prepared by electrospinning at appropriate temperatures and cross-linked by visible-light-mediated photoirradiation. Fibers in the diameter range of 300 nm−1.5 μm were produced. Fabrics were found to have an average pore size of 78 μm. The occurrence of cross-linking was confirmed by ^{13}C solid-state NMR with a commensurate increase in modulus.

Introduction

Elastomeric proteins are widely distributed among a diverse range of animal species and tissues where they have evolved precise structures to perform specific biological functions. These proteins, which include for example abductin,[1] tropoelastin,[2−4] bysuss,[5] silk,[6,7] and titin, all possess rubberlike elasticity, undergoing high deformation without rupture, storing energy involved in deformation, and then recovering to their original state when the stress is removed. The ability of proteins to exhibit rubberlike elasticity relates to both their primary and secondary structure as well as to those features such as protein self-assembly and other intermolecular interactions that dictate the formation of true or virtual networks. Specifically, all elastomeric materials must satisfy two criteria. First, to respond quickly to an applied force, the monomers, which in elastomeric proteins typically consist of repetitive glycine-rich peptide motifs, must be flexible and conformationally free. Second, elastomeric macromolecules must be cross-linked to form a network. Characteristically, elastic proteins combine highly mobile domains with domains that form covalent or noncovalent cross-links. Thus, the size and properties of the mobile domains and the degree of cross-linking can influence the elastic behavior of protein-based materials.

Elastin, which is derived from the soluble precursor tropoelastin, is widely distributed in vertebrate tissues where it consists of highly mobile repetitive glycine-rich hydrophobic domains of variable length that alternate with alanine-rich, lysine-containing domains that form cross-links.[3,4,8] Native elastin's intrinsic insolubility, however, has largely limited its capacity to be purified and processed into forms suitable for biomedical or industrial applications. Recently, this limitation has been largely overcome, in part, by the structural characterization of the mobile domains. Specifically, comprehensive sequence analysis has revealed the presence of consensus tetrapeptide (Val-Pro-Gly-Gly), pentapeptide (Val-Pro-Gly-Val-Gly), and hexapeptide (Ala-Pro Gly-Val-Gly-Val) repeat motifs.[2,9−14] Notably, only polymers of the pentapeptide exhibit elastic behavior with spectroscopic features, including a highly mobile backbone and the presence of β-turns and a loose helical β-spiral, that are consistent with those of native elastin.[15,16] Thus, the pentapeptide sequence (VPGVG) has formed the basis for the synthesis of protein polymers with elastomeric domains by standard solution and solid-phase chemical methodologies and, more recently, by genetic engineering strategies.[17−21]

In its native form, elastin is present as a network of elastic fibers that are cross-linked through available lysine residues found in interspersed alanine-rich regions.[22−25] Characteristically, cross-linking occurs in the solid state, that is, after cellular secretion of tropoelastin with local fiber deposition. In this fashion, the biostability of elastin is enhanced and its mechanical properties are modulated. In contrast, cross-linking of synthetic elastin−mimetic protein polymers has been largely investigated in solution phase systems using either γ-irradiation,[26] chemical, or enzymatic-based approaches.[27] For example, Urry et al.[4] have demonstrated the feasibility of generating tubular hydrogels by γ-irradiation-mediated cross-linking, and Welsh et al.[28] have used glutaraldehyde to cross-link an elastin−mimetic protein film. While these approaches do provide a measure of control over the degree of cross-linking, the chemical nature as well as the location of the cross-link is often ill-defined. Furthermore, none of these reaction schemes are appropriate for heterogeneous multicomponent systems in which there may be a need

[†] Department of Surgery, Emory University.
[‡] School of Textile Engineering, Georgia Institute of Technology.
[§] Department of Chemistry, Emory University.
[⊥] Department of Bioengineering, Emory University.
[#] Chemical Engineering, Georgia Institute of Technology.
* Corresponding author: phone (404) 727-8413; Fax (404) 727-3660; e-mail echaiko@emory.edu.

10.1021/ma011429t CCC: $22.00
Published on Web 01/29/2002

either to control the degree of cross-linking among individual constituents or otherwise to incorporate elements within the structure that may be adversely affected by unintended side reactions. In summary, the approaches that have been described to date have provided important insights into the physiochemical behavior of bioelastic systems under a variety of environmental conditions and have led to novel processing strategies for creating elastomeric hydrogels for drug delivery and other applications. However, we believe that the generation of meaningful constructs for the engineering of human tissues and artificial organs will require the processing of elastomeric protein polymers into fibers and fabrics in which the protein polymer forms a cross-linked network. Thus, it is desirable to utilize a cross-linking strategy that is efficient in the solid state, achieves precise control over the nature and degree of cross-linking, and facilitates spatial and temporal control over the reaction process.

In a previous communication,[29] we have described the optimization of an electrospinning process to produce uniform nanofibers ($\phi < 1\ \mu$m) and nonwoven fabrics of an elastin protein polymer poly((Val-Pro-Gly-Val-Gly)$_4$-(Val-Pro-Gly-Lys-Gly))$_{39}$. Notably, amino acid substitutions in the fourth position of the pentapeptide does not affect the formation of a β-spiral,[30−32] which is critical for the biomechanical behavior of elastin analogues. Thus, the incorporated lysine group (LYS-24) provides an amino functionality that can be conveniently utilized for polymer cross-linking. Indeed, McMillan et al.[21] have recently reported the formation of structurally well-defined cross-linked elastin−mimetic hydrogels using an *N*-hydroxysuccinimide ester of a bifunctional carboxylic acid, specifically, disuccinimidyl suberate, as cross-linker of available amino groups in the solution phase. In this report, we describe the incorporation of functional groups into the protein polymer backbone that facilitate site-specific solid-state photo-cross-linking using either UV or visible light actived photoinitiators. Significantly, this approach provides for both spatial and temporal control over the cross-linking reaction. The generation of cross-linked elastin−mimetic fibers and films is reported, and mechanical properties are characterized.

Experimental Section

Materials. Methacrylic anhydride, eosin Y (EY, 5 wt % in water), triethanolamine (TEA), and 1-vinyl-2-pyrrolidinone (VP) were obtained from Aldrich and used as received. A standard photoinitiator solution was prepared according to compositions published elsewhere.[33] The solution composition was 10 mM EY, 225 mM TEA, and 37 mM VP. Dialysis was conducted using a Spectra/pro membrane (MWCO 6000−8000) obtained from VWR Scientific.

An elastin−mimetic protein polymer, poly((-Val-Pro-Gly-Val-Gly-)$_4$(-Val-Pro-Gly-Lys-Gly-))$_{39}$, of molecular weight 81 kDa was synthesized by a recombinant genetic engineering method, the details of which have been reported elsewhere.[20,21,34] Briefly, a concatameric gene of 3000 base pairs was isolated that encoded a repetitive polypeptide comprising 39 repeats of the elastin−mimetic sequence. The protein polymer was expressed from recombinant plasmid pRAM1 in *E. coli* strain BLR(DE3) under isopropyl β-thiogalactopyranoside induction and purified to a high yield (64 mg/L) by reversible, temperature-induced precipitation from the cell lysate. The sequence of the protein polymer has been confirmed by automated Edman degradation and MALDI-TOF mass spectroscopy of site-specific proteolytic cleavage fragments. Structural analysis of this recombinant protein has also included SDS PAGE as well as ^{1}H and ^{13}C NMR.[20,21]

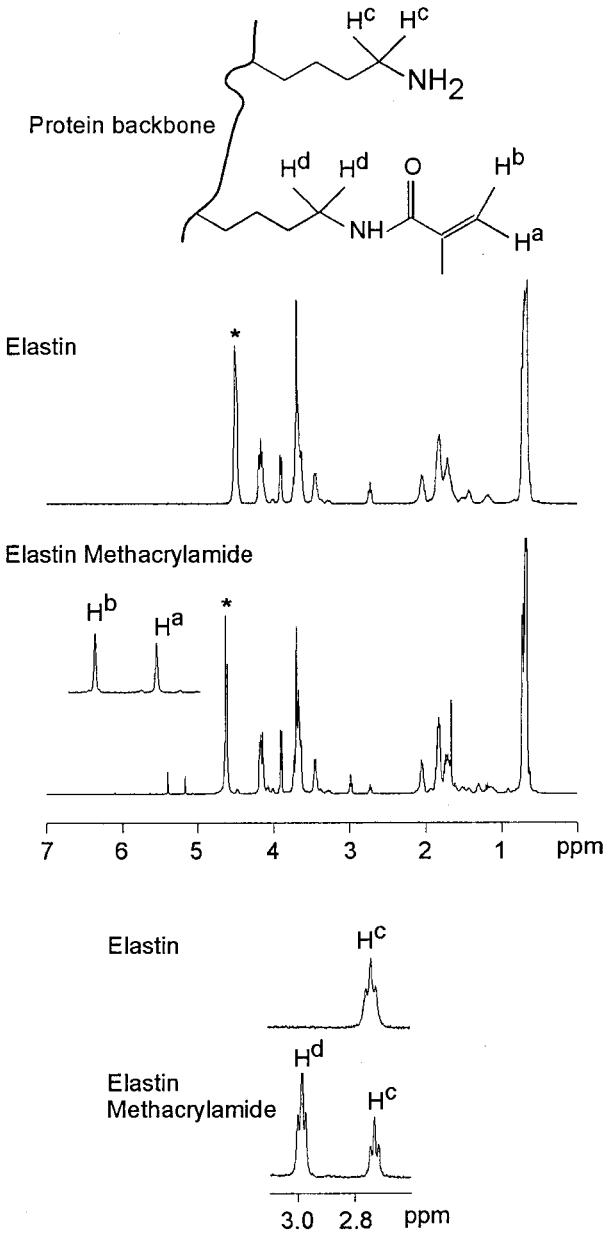

Figure 1. (a) ^{1}H NMR spectra of elastin and elastin methacrylamide measured in D_2O (*) at room temperature. Expanded region of the protons corresponding to the double bonds (H^a, H^b) is also shown for the elastin methacrylamide spectrum. (b) Expanded version of the figure between 2.6 and 3.1 ppm. The spectra indicate the shift in the methylene protons α to the amino group prior (H^c) and subsequent (H^d) to the reaction of the elastin analogue with methacrylic anhydride.

Synthesis of Methacrylate-Modified Elastin. The procedure for acrylate modification of amino-containing compounds developed by Van den Bulcke et al.[35] was followed. The elastin−mimetic protein polymer was dissolved in pH 7.5 phosphate buffer solution and cooled to 5 °C, and an excess of methacrylic anhydride was added. The reaction was allowed to proceed for 8 h, after which the reaction mixture was diluted and dialyzed against distilled water at room temperature for 48 h with frequent changes of the dialyzate solution.

Instrumentation. All ^{1}H NMR spectra were recorded at room temperature on a Bruker AMX 500 spectrometer operating at a ^{1}H resonance frequency of 500 MHz. Thirty-two scans were acquired for signal-to-noise averaging. A recycle delay of 30 s was used to ensure quantitative spectra. In all cases D_2O was used as the internal standard, and a concentration of 10 mg/mL was employed.

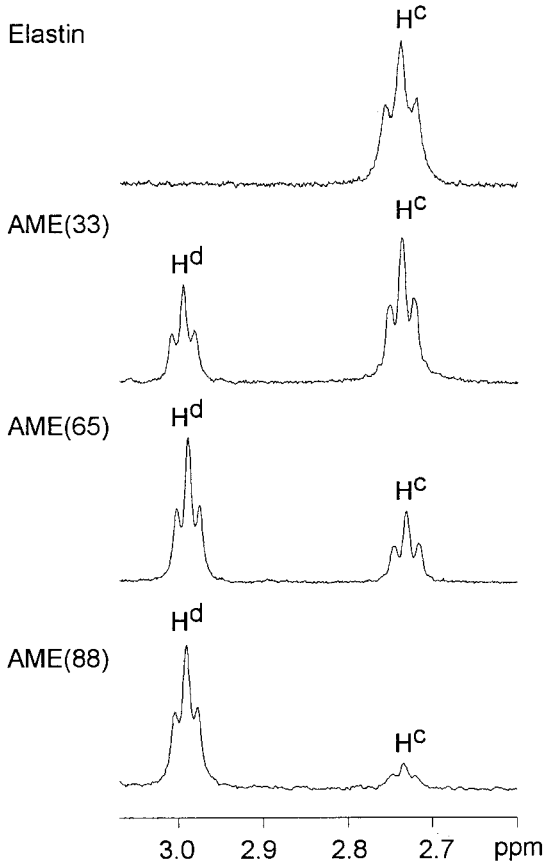

Figure 2. ^{1}H NMR spectra of elastin and AME. The DOF of AME's is provided in parentheses. The expanded portion of the spectra between 2.6 and 3.1 ppm is shown. As DOF increases, the H^d peak grows in intensity at the expense of the H^c peak. The DOF can be computed from the intergrated intensities of the H^c and H^d peaks.

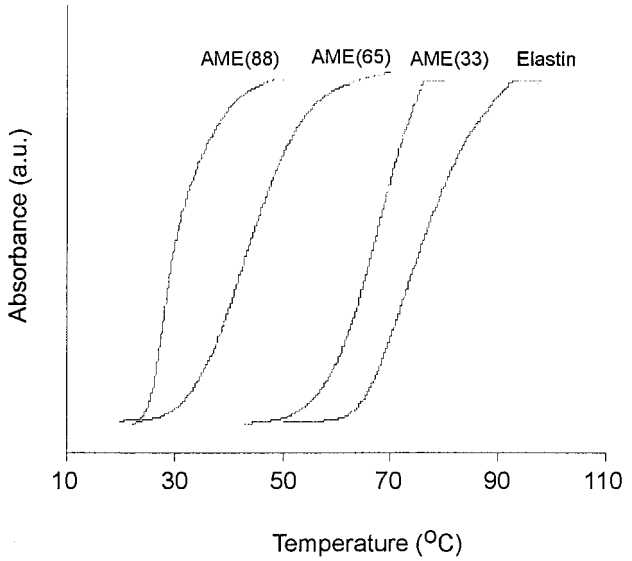

Figure 3. Temperature-dependent turbidimetry data for elastin and acrylate-modified elastin with different degrees of functionalization. The inverse transition temperature (T_t) decreases with increase in the degree of functionalization (DOF). DOF dictates the temperature (processing window) at which fibers can be formed from aqueous solutions. The temperature window to the left of T_t is amenable for fiber formation.

All solid-state NMR experiments were conducted at room temperature on a Bruker DSX 300 spectrometer operating at a ^{1}H resonance frequency of 300 MHz in a Bruker double-

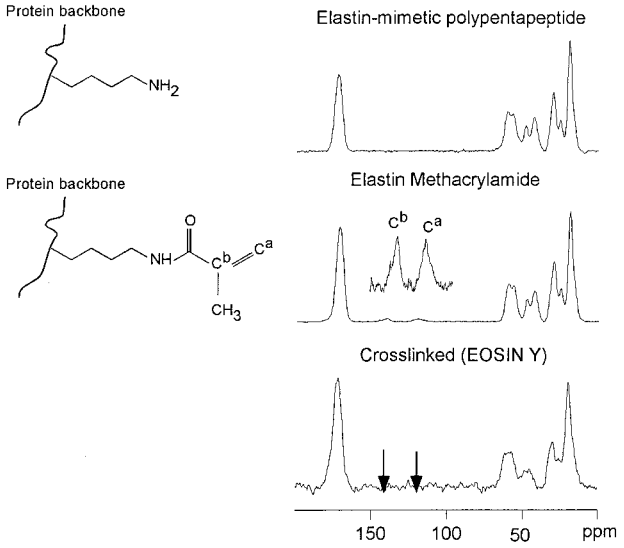

Figure 4. ^{13}C CP/MAS/TOSS spectra of an elastin−mimetic protein polymer, methacrylate-modified elastin, and cross-linked elastin recorded at room temperature (23 °C). Contact time = 1 ms and spinning speed ($\omega_r/2\pi$) = 5 kHz. The disappearance of the peaks C^a and C^b in the spectrum for the cross-linked material indicates cross-linking after exposure to visible light.

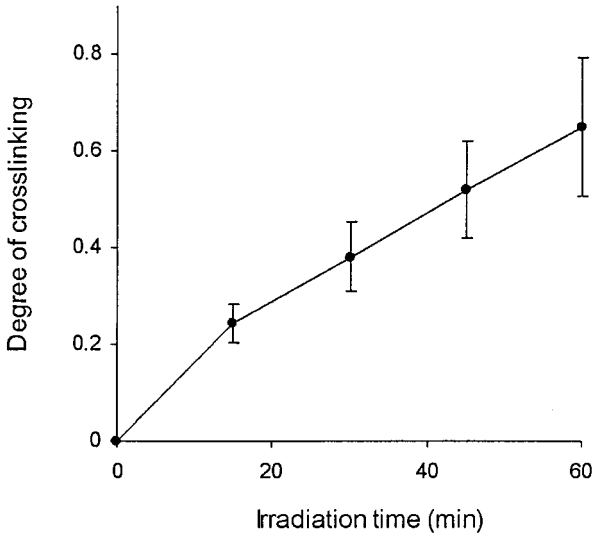

Figure 5. Degree of cross-linking of AME(65) determined by ^{13}C solid-state NMR as a function of irradiation time. Data presented as mean ± standard deviation.

resonance MAS probehead. A standard cross-polarization (CP) pulse sequence was employed under conditions of magic angle spinning (MAS). A spinning speed of 5 kHz was employed. A TOSS sequence was used in conjunction with CP to provide a spectrum free of spinning sidebands.[36,37] A 4.5 μs ^{1}H 90° pulse, a 1 ms contact time, a 9 μs ^{13}C 180° pulse, and a 3 s recycle delay were employed with 5000−16 000 scans accumulated for signal averaging. All diffusion NMR experiments were performed in a Bruker DSX-400 spectrometer operating at a ^{1}H resonance frequency of 400 MHz using a standard Bruker microimaging accessory. A stimulated echo pulse sequence[37] was used to determine the behavior of fluids trapped in materials. Diffusion times of up to 1000 ms were employed, and the field gradient was varied between 0 and 95 G/cm. The gradients had been calibrated by running a PFG-STE experiment of distilled water and adjusting the calibration so that the data would fit the diffusion coefficient of pure water. A recycle delay of 5 s was employed to achieve magnetization equilibrium. Diffusion data were recorded as a function of gradient strength and diffusion time. For determining pore

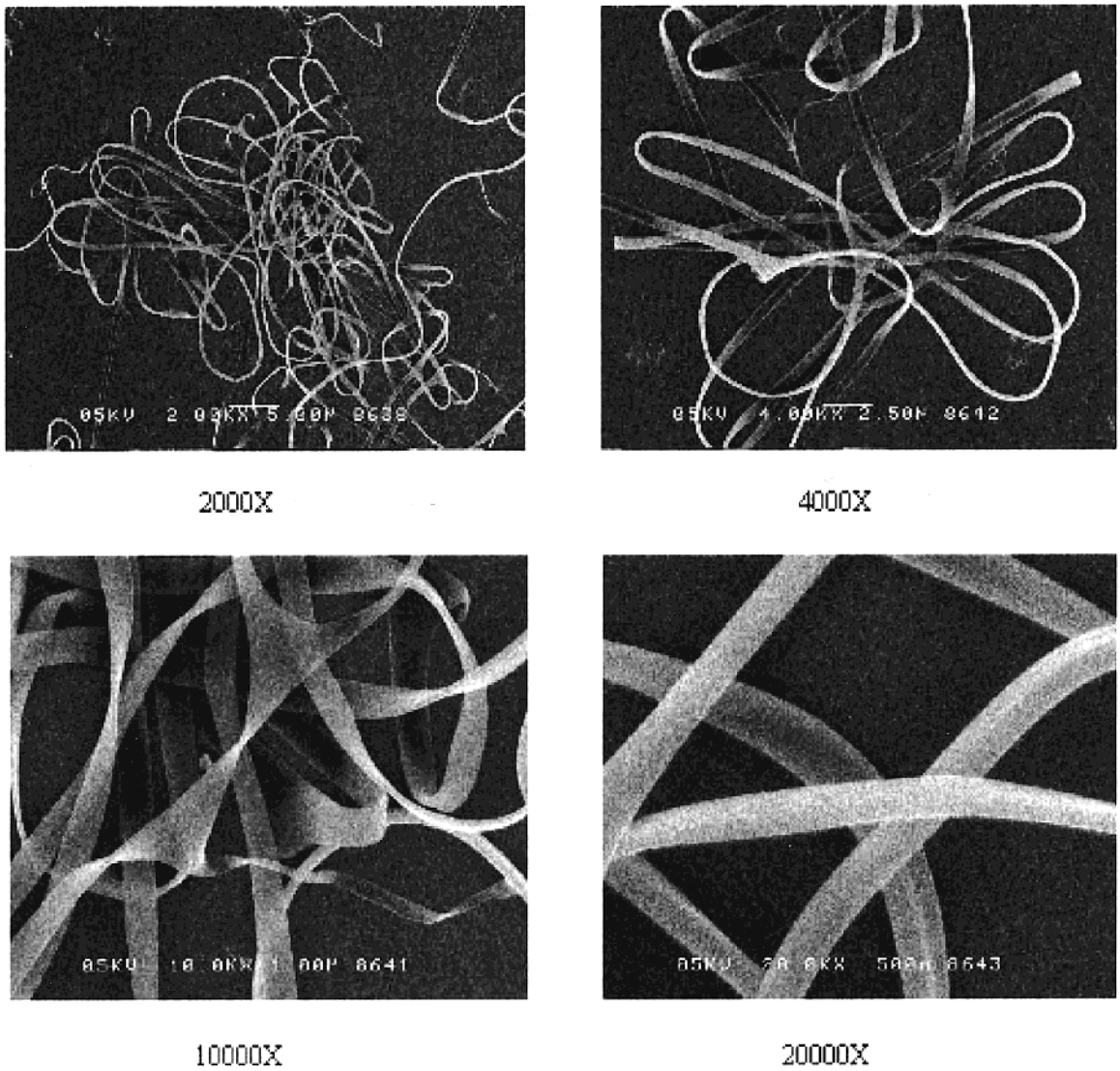

Figure 6. SEM micrographs of fibers spun from a 10 wt % AME(65) solution at room temperature. Flow rate = 50 μL/min; photoinitiator = EY (3 wt % of protein content). Long uniform fibers are produced with occasional triangle type bifurcation points. Fibers in the diameter range from 300 to 500 nm were produced.

sizes the fabrics were cut into circular specimens and immersed in water containing 0.1% Triton X prior to the measurement.

Temperature-dependent turbidimetry measurements were recorded in an Ultrospec 3000 UV/vis spectrophotometer equipped with a programmable Peltier cell and temperature control unit from Amersham Pharmacia Biotech, Inc. (Piscataway, NJ). Inverse temperature transitions (T_t), which represent the lower critical solution temperatures (LCST) of the elastin−mimetic protein polymer and its acrylate modified analogues, were monitored in water (concentration of 0.5−0.7 mg/mL) at 280 nm.

An in-lens field emission scanning electron microscope (ISI DS-130F Schottky field emission SEM) was used and operated at 5 or 25 kV. High-definition topographic images at low (~1000×) and medium (30 000×) magnifications and high resolution and high-magnification images (≥100 000×) were digitally recorded with very short dwell times and without beam-induced damage. Fiber samples were deposited onto silicon chips for SEM studies. The silicon chips were subsequently mounted onto aluminum specimen stubs with silver paste, degassed for 30 min, and coated with a 1 nm chromium (Cr) ultrathin film using a Denton DV-602 Turbo magnetron sputter system.

Visible light irradiation was performed using a DynaLume quartz halogen illuminator equipped with a heat shield obtained from Scientific Instruments.

A miniature materials tester Minimat 2000 (Rheometric Scientific) was used to determine the tensile properties. The machine was used in the tensile deformation mode with a 20 N load cell and a strain rate of 1 mm/min. Fabric samples (10 mm × 1.5 mm × 0.05 mm) were used as test specimens with a gauge length of 8 mm. For testing under hydrated conditions, test samples were hydrated at 37 °C for 1 h, and excess water was removed prior to measurement by squeezing the sample between a tissue. For each sample, eight specimens were tested, and average modulus and tensile strength values were determined.

Fiber Spinning. Elastin−mimetic peptide polymers were spun into fibers using an electrospinning technique, as detailed elsewhere.[29] Briefly, peptide polymer solutions (10−15 wt %) were prepared in ultrafiltered grade, distilled, deionized water (18 MΩ·cm, Continental) by mixing for 12 h at 4 °C. With the aid of a syringe pump (Harvard Apparatus, Inc.), the solution was extruded at ambient temperature and pressure and at a defined flow rate through a positively charged metal blunt tipped 22 gauge needle (0.0253 in. × 1.5 in.). The needle was connected to a 1 mL syringe using Tygon tubing (1.6 mm i.d.). Fibers were collected on a grounded aluminum plate located 15 cm below the tip of the needle. A high-voltage, low-current power supply (ES30P/DDPM, Gamma High Voltage Research, Inc.) was utilized to establish an electric potential of 18 kV.

Nonwoven fabric samples were produced by electrospinning elastin methacrylate solutions for extended periods of time.

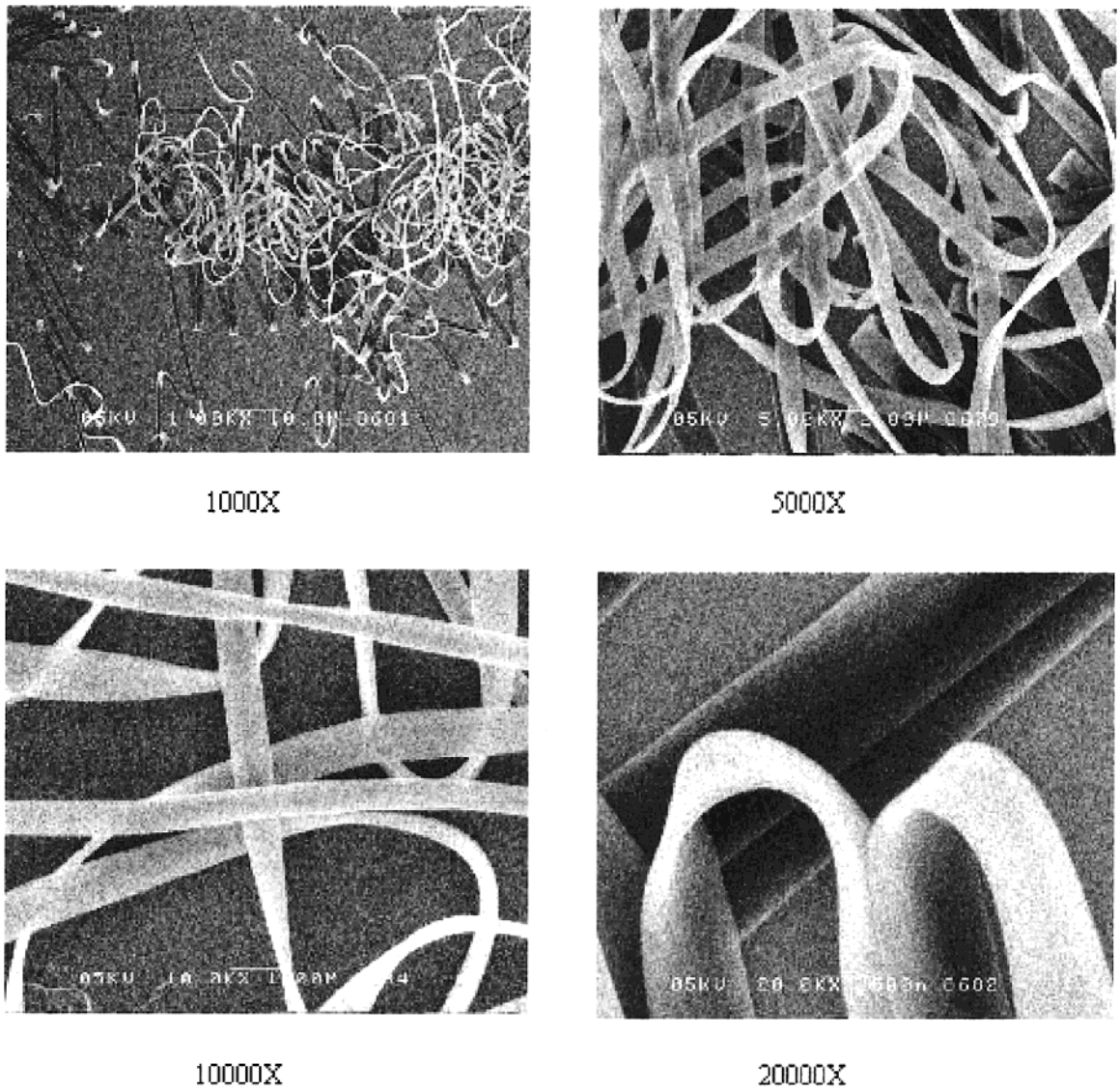

Figure 7. SEM micrographs of fibers spun from a 15 wt % AME(65) solution at room temperature. Flow rate = 50 μL/min; photoinitiator = EY (3 wt % of protein content). Long uniform fibers are produced with a flattened or ribbon-shaped morphology. Fibers in a variety of diameter ranges are produced (typically from 300 nm to 1.5 μm).

The apparatus was modified to include a rotating mandrel to produce fabric samples. The fabric samples were collected on an aluminum foil wrapped around the grounded mandrel placed at a prescribed horizontal distance with respect to the charged tip of the needle.

Results and Discussion

Acrylate Derivatization of an Elastin−Mimetic Protein Polymer. ^{1}H NMR spectra of the elastin−mimetic protein polymer and its acrylate-modified analogue (AME) recorded at room temperature in D_2O are shown in Figure 1. The spectrum of the acrylate-modified material expanded between 5.0 and 5.7 ppm confirms incorporation of the double bonds through peaks at 5.3 (H^a) and 5.6 ppm (H^b). Notably, acrylate modification produces a 0.25 ppm (H^d) downfield shift of the methylene protons α to the amino group (H^c). Thus, a convenient means of calculating the degree of functionalization (DOF) is established by dividing the integrated intensity of the 3 ppm peak by the sum of the integrated intensities of both the 3 and 2.75 ppm peaks. As anticipated, the degree of functionalization depends on the molar reactant ratio of methacrylic anhydride to peptide polymer, with an increase in DOF of 33% to 88% observed upon increasing the ratio from 1:1 to 3:1 (Figure 2). This provides the ability to generate materials having a wide range of mechanical properties after cross-linking. For the remainder of the discussion, AME's will be represented by their respective DOF in parentheses.

Inverse Temperature Transitions of Acrylate-Modified Elastin Analogues. Mutual compatibility of a polymer and a solvent has been extensively studied and is often critical for processing needs. Urry et al.[16] have shown that protein polymers based on the VPGVG repeat sequence have an inverse temperature transition with phase separation observed on increasing solution temperature. Characteristically, inverse transition temperatures (T_t) can be determined by temperature-dependent turbidimetry measurements with T_t defined as the temperature corresponding to one-half maximal turbidity. The data demonstrate that acrylate modification causes a reduction in T_t with a reduction of approximately 50 °C noted for analogues with a DOF of 88% (Figure 3). Prior investigations have established that an increase in the hydrophobicity of model VPGVG protein polymers, as a result of substitution at the

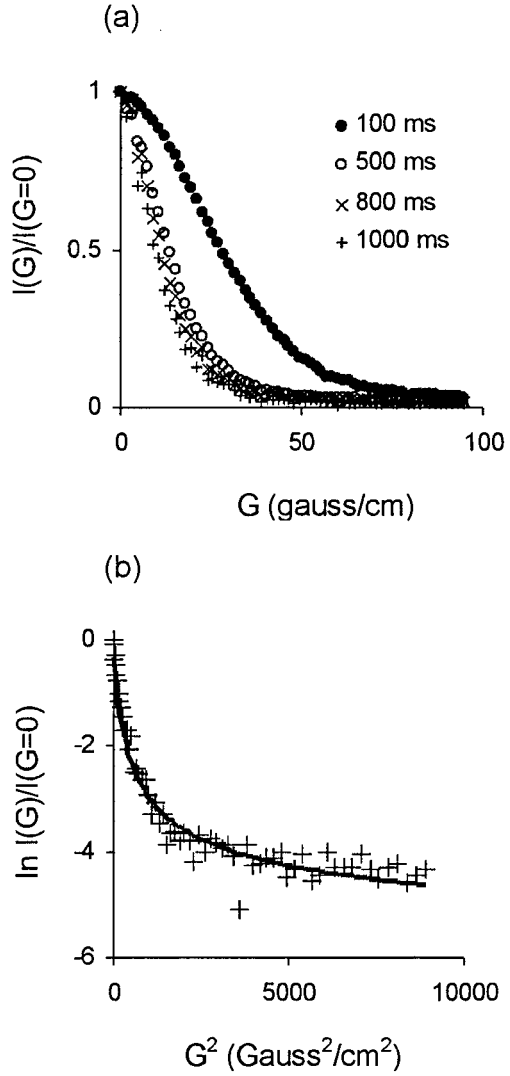

Figure 8. (a) Diffusion NMR data for a fabric sample made from AME(65) as a function of diffusion time. (b) Fit shown for a Gaussian distribution of pore sizes on the 1000 ms diffusion data. Average pore diameter was found to be 78 μm.

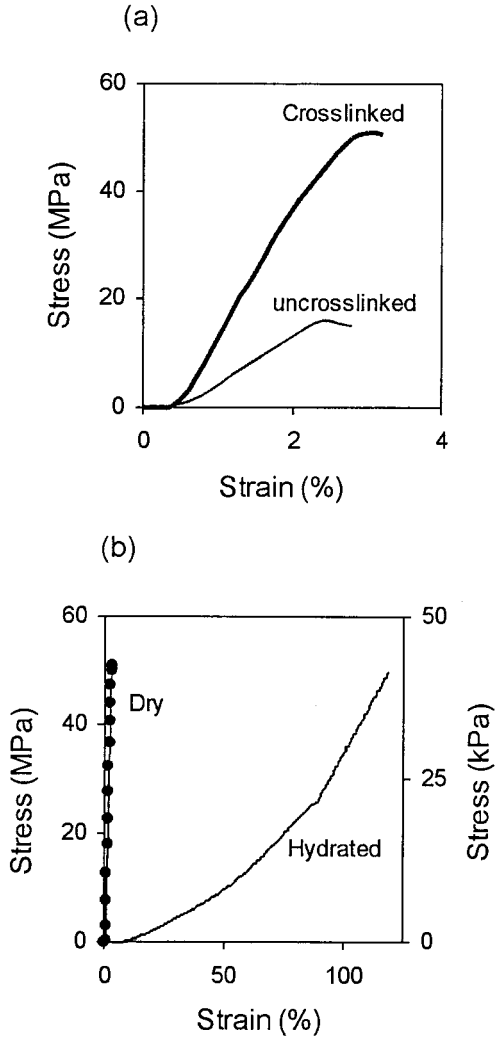

Figure 9. (a) Representative stress−strain curves of cross-linked and un-cross-linked fabric samples of AME(65) in the dry state. Cross-linking increases both tensile strength and modulus of the sample. (b) Representative stress−strain curves of dry (●) and hydrated cross-linked AME(65) fabric samples measured at a strain rate of 1 mm/min at room temperature.

fourth position, would be thermodynamically offset with a decrease in the transition temperature.[4] Significantly, in our studies the processing temperature for fiber formation is dictated by T_t. For example, fibers can be spun from aqueous solutions of AME(33) and AME(65) at room temperature, which is well below their T_t. However, the onset of turbidity begins close to room temperature for AME(88). Thus, fibers from 10 to 15 wt % AME(88) in water required cold room spinning at 5 °C. For the remainder of the discussion all experiments were conducted on AME(65) since it afforded spinnable solutions at room temperature.

Cross-Linking Efficiency in the Solid State. The dependence of protein cross-linking on irradiation time was investigated in detail for the 15 wt % AME(65)/photoinitiator system using ^{13}C solid-state NMR.[38,39] Dry film samples were irradiated for up to 60 min and stored prior to solid-state NMR analysis in brown bottles at −20 °C. After an hour of visible light irradiation at 70 mW/cm^2, the cross-linking process was complete as evidenced by the disappearance of double bonds (Figure 4). ^{13}C solid-state NMR spectra were then acquired for samples irradiated for varying lengths of time (15−60 min) to establish a correlation between irradiation time and degree of cross-linking (Figure 5). The double bond region between 110 and 150 ppm was integrated in each of these spectra and was normalized with respect to the intensity of the carbonyl peak around 172 ppm. The degree of cross-linking (DOC) was then computed using

$$\mathrm{DOC}(t) = 0.65\left(1 - \frac{I_{110-150}(t)}{I_{110-150}(t=0)}\right)$$

where t is the irradiation time, I the integrated intensity of the double bond region normalized with respect to the carbonyl peak, and the factor 0.65 is the degree of functionalization of the AME.

Morphology of Electrospun Elastin−Mimetic Fibers and Fiber Networks. Prior studies have demonstrated that electrospinning provides a convenient approach for generating submicron diameter fibers from an elastin−mimetic protein polymer. In the current investigation, no appreciable effect on fiber morphology was observed following acrylate modification or the addition of photoinitiator to the spinning solution. At a flow rate of 50 μL/min, spinning a 10 wt % AME-(65) solution produced long uniform fibers with diam-

eters ranging between 300 and 500 nm with occasional trifurcation points noted (Figure 6). On increasing the solution concentration of protein polymer to 15 wt % solution, a predominantly flat or ribbon type morphology was observed (Figure 7).

The porosity of scaffolds is considered a key feature essential to the growth and migration of cells. The porosity of fabric networks produced by electrospinning was determined using the ^{1}H PFG NMR diffusion technique, the details of which regarding special aspects for the characterization of fibrous structures have been reported elsewhere.[40] Figure 8a shows the diffusion data measured as a function of the magnetic field gradient strength (G) for varying lengths of diffusion time. The data measured at diffusion time of $\Delta = 800$ ms and $\Delta = 1000$ ms can be considered identical, indicating that the time limit is reached where the diffusion experiment is probing the structure of fluids confined in pores.[41] The 1000 ms diffusion data were used to determine the pore size. In Figure 8b the logarithm of the normalized intensity is plotted as a function square of the gradient strength. In the case where the pore sizes are uniform, a plot of normalized logarithm of measured intensities vs G^2 would be linear with a slope that is related to the square of the pore size.[41] The plot is clearly nonlinear, suggesting a distribution of pore sizes. To determine an average pore size, one can use any distribution that is realistic and fits the data well. A Gaussian distribution of pore sizes has been employed here.

$$\ln \frac{I(G)}{I(G=0)} = -\frac{\alpha^2 {R_0}^2}{1+\sigma^2\alpha^2} - \frac{1}{2}\ln(1+\sigma^2\alpha^2)$$

The mathematical relationship between the diffusion profile and the pore radius in the case of a Gaussian distribution of pore sizes has already been determined by Callaghan et al.[42] with α^2 given by

$$\alpha^2 = \frac{\gamma^2\delta^2 G^2}{5}$$

where $I(G)$ is the intensity at a gradient strength G, γ the gyromagnetic ratio, R_0 the mean pore radius, σ^2 twice the variance of the distribution, and δ the time length of each gradient pulse (1 ms). For all pore radii covered by the Gaussian distribution the condition $\Delta > {R_0}^2/6D$ should be fulfilled if the above equation is to be valid. Figure 8b also shows the fit using above equation to the 1000 ms data. Data fitting was done using the IGOR Pro software package (Wavemetrics, Lake Oswego, OR). From the fit, an average pore size of 78 μm with a standard deviation of 44 μm was obtained. This pore size is within the range reported for other porous scaffolds.[43−45]

Mechanical Behavior of a Fiber Network Produced from an Elastin−Mimetic Protein Polymer. In the dry state, cross-linking renders fiber network samples stiffer and more brittle. For example, nonwoven fabrics composed of un-cross-linked AME(65) exhibited a Young's modulus of 0.7 ± 0.15 GPa and a tensile strength of 16.2 ± 6.3 MPa, while cross-linked samples had a modulus of 1.8 ± 0.4 GPa and a tensile strength of 43.3 ± 5.2 MPa (Figure 9a). Thus, cross-linking enhanced both Young's modulus and tensile strength with a concomitant decrease in the strain to failure from 3.9 ± 0.2% to 2.3 ± 0.35%. Upon hydration, the average modulus decreased to 0.45 ± 0.08 MPa with a substantial increase in strain to failure to 105 ± 8% (Figure 9b). These values are comparable to those published for native elastin. Notably, the degree of cross-linking (DOC) estimated from ideal rubber elasticity theory ($0.43 < \mathrm{DOC} < 0.62$) compares well with that obtained from solid-state NMR measurements ($0.51 < \mathrm{DOC} < 0.65$).

Conclusions

Postprocessing solid-state cross-linking of elastin−mimetic fibers was investigated. Through available lysine residues, an elastin−mimetic protein polymer was modified to incorporate an acrylate moiety. The degree of acrylate functionalization could be varied by changing the reactant ratio of anhydride to elastin. The AME's were found to have lower inverse transition temperature than the unmodified sample. This was attributed to the increase in the hydrophobicity of the sample with the introduction of the acrylate group. The inverse transition temperature in turn dictated the temperature for fiber formation. Fibers and fabric samples of AME were prepared by electrospinning at appropriate temperatures. Depending upon the concentration of the solution, fibers with diameter ranging from 300 nm to 1.5 μm were produced. The fibers were subsequently cross-linked using photoirradiation.

The insolubility of the resulting sample in water indicated a high degree of cross-linking with complete cross-linking confirmed by ^{13}C solid-state NMR and mechanical measurements. The mechanical properties of the samples were commensurate with that expected, in that modulus and tensile strength increased upon cross-linking in the dry state. Moreover, hydrated samples displayed rubberlike behavior with high extensibility. Thus, acrylate modification provides a viable route for solid-state cross-linking of elastin−mimetic protein-based materials. These fabric networks were found to have porosities in the same range as those exhibited by other porous scaffolds. With the production of cross-linked elastin−mimetic fabrics, the capacity to engineer tissuelike constructs has been significantly enhanced.

Acknowledgment. This work was supported by the NSF Center for the Engineering of Living Tissues, EEC-9731643, and grants from the NIH. The authors acknowledge Dr. Suri Iyer and Dr. V. E. Narayanaswamy for assistance with NMR measurements.

References and Notes

(1) Cao, Q.; Wang, Y.; Bayley, H. *Curr. Biol.* **1997**, *7*, R677−8.
(2) Gray, W. R.; Sandberg, L. B.; Foster, J. A. *Nature (London)* **1973**, *246*, 461−6.
(3) Sandberg, L. B.; Soskel, N. T.; Leslie, J. G. *N. Engl. J. Med.* **1981**, *304*, 566−579.
(4) Urry, D. W.; Luan, C.-H.; Harris, C. M.; Parker, T. M.; McGrath, K.; Kaplan, D., Ed.; Birkhauser: Boston, 1997; pp 133−177.
(5) Deming, T. J. *Curr. Opin. Chem. Biol.* **1999**, *3*, 100−5.
(6) Hayashi, C. Y.; Shipley, N. H.; Lewis, R. V. *Int. J. Biol. Macromol.* **1999**, *24*, 271−5.
(7) Hayashi, C. Y.; Lewis, R. V. *J. Mol. Biol.* **1998**, *275*, 773−84.
(8) Indik, Z.; Yeh, H.; Ornstein-Goldstein, N.; Sheppard, P.; Anderson, N.; Rosenbloom, J. C.; Peltonen, L.; Rosenbloom, J. *Proc. Natl. Acad. Sci. U.S.A.* **1987**, *84*, 5680−4.
(9) Urry, D. W.; Mitchell, L. W.; Ohnishi, T. *Biochim. Biophys. Acta* **1975**, *393*, 296−306.
(10) Sandberg, L. B.; Gray, W. R.; Foster, J. A.; Torres, A. R.; Alvarez, V. L.; Janata, J. *Adv. Exp. Med. Biol.* **1977**, *79*, 277−84.

(11) Khaled, M. A.; Renugopalakrishnan, V.; Urry, D. W. *J. Am. Chem. Soc.* **1976**, *98*, 7547−53.
(12) Rapaka, R. S.; Okamoto, K.; Urry, D. W. *Int. J. Pept. Protein Res.* **1978**, *11*, 109−27.
(13) Urry, D. W.; Harris, R. D.; Long, M. M.; Prasad, K. U. *Int. J. Pept. Protein Res.* **1986**, *28*, 649−60.
(14) Broch, H.; Moulabbi, M.; Vasilescu, D.; Tamburro, A. M. *J. Biomol. Struct. Dyn.* **1998**, *15*, 1073−91.
(15) Urry, D. W.; Cunningham, W. D.; Ohnishi, T. *Biochemistry* **1974**, *13*, 609−16.
(16) Urry, D. W.; Trapane, T. L.; Prasad, K. U. *Biopolymers* **1985**, *24*, 2345−56.
(17) McPherson, D. T.; Morrow, C.; Minehan, D. S.; Wu, J.; Hunter, E.; Urry, D. W. *Biotechnol. Prog.* **1992**, *8*, 347−52.
(18) McPherson, D. T.; Xu, J.; Urry, D. W. *Protein Expression Purif.* **1996**, *7*, 51−7.
(19) Panitch, A.; Yamaoka, T.; Fournier, M. J.; Mason, T. L.; Tirrell, D. A. *Macromolecules* **1999**, *32*, 1701−1703.
(20) McMillan, R. A.; Lee, T. A. T.; Conticello, V. P. *Macromolecules* **1999**, *32*, 3643−3648.
(21) McMillan, R. A.; Conticello, R. P. *Macromolecules* **2000**, *33*, 4809−4821.
(22) Robins, S. P. *Methods Biochem. Anal.* **1982**, *28*, 329−79.
(23) Miyoshi, M.; Kanamori, M.; Rosenbloom, J. *J. Biochem. (Tokyo)* **1976**, *79*, 1235−43.
(24) Franzblau, C.; Foster, J. A.; Faris, B. *Adv. Exp. Med. Biol.* **1977**, *79*, 313−27.
(25) Akagawa, M.; Suyama, K. *Connect. Tissue Res.* **2000**, *41*, 131−141.
(26) Zhang, H.; Prasad, K. U.; Urry, D. W. *J. Protein Chem.* **1989**, *8*, 173−82.
(27) Kagan, H. M.; Tseng, L.; Trackman, P. C.; Okamoto, K.; Rapaka, R. S.; Urry, D. W. *J. Biol. Chem.* **1980**, *255*, 3656−9.
(28) Welsh, E. R.; Tirrell, D. A. *Biomacromolecules* **2000**, *1*, 23−30.
(29) Huang, L.; McMillan, R. A.; Apkarian, R. P.; Pourdeyhimi, B.; Conticello, V. P.; Chaikof, E. L. *Macromolecules* **2000**, *33*, 2989.
(30) Thomas, G. J. J.; Prescott, B.; Urry, D. W. *Biopolymers* **1987**, *26*, 921−934.
(31) Chang, D. K.; Venkatachalarn, C. M.; Prasad, K. U.; Urry, D. W. *J. Biomol. Struct. Dyn.* **1989**, *6*, 851−858.
(32) Urry, D. W.; Chang, D. K.; Krishna, N. R.; Huang, D. H.; Trapane, T. L.; Prasad, K. U. *Biopolymers* **1989**, *28*, 819−833.
(33) Cruise, G. M.; Hegre, O. D.; Scharp, D. S.; Hubbell, J. A. *Biotechnol. Bioeng.* **1998**, *57*, 655.
(34) McMillan, R. A.; Caran, K. L.; Apkarian, R. A.; Conticello, V. P. *Macromolecules* **1999**, *32*, 9067−9070.
(35) Van Den Bulcke, A. I.; Bogdanov, B.; De Rooze, N.; Schacht, E. H.; Cornelissen, M.; Berghmans, H. *Biomacromolecules* **2000**, *1*, 31.
(36) Dixon, W. T. *J. Chem. Phys.* **1982**, *77*, 1800.
(37) Dixon, W. T.; Schaefer, J.; Sefcik, M. D.; Stejskal, E. O.; McKay, R. A. *J. Magn. Reson.* **1982**, *49*, 341.
(38) O'Donnell, J. H.; Whittaker, A. K. *Radiat. Phys. Chem.* **1992**, *36*, 209.
(39) O'Donnell, J. H.; Whittaker, A. K. *J. Polym. Chem. Ed.* **1992**, *30*, 185.
(40) Leisen, J.; Beckham, H. W. Leonas, K. K. TANDEC, 9th Annual Nonwovens Conference, Chapter 5.1, 1999.
(41) Callghan, P. *Principles of Nuclear Magnetic Resonance Microscopy*; Clarendon: Oxford, 1991.
(42) Callaghan, P. T.; Jolley, K. W.; Humprey, R. S. *J. Colloid Interface Sci.* **1983**, *93*, 521.
(43) von Heimburg, D.; Zachariah, S.; Kuhling, H.; Heschel, I.; Schoof, H.; Hafemann, B.; Pallua, N. *Biomaterials* **2001**, *22*, 429.
(44) Mikos, A. G.; Temenoff, J. S. *EJB: Electron. J. Biotechnol.* [online] **2000**, *3* (2). Available from http://www.ejb.org/content/vol3/issue2/full/5/index.html.
(45) Pieper, J. S.; Van Wachem, P. B.; Van Luyn, M. J. A.; Brouwer, L. A.; Hafmans, T.; Veerkamp, J. H.; Van Kuppevelt, T. H. *Biomaterials* **2000**, *21*, 1689.

MA011429T